Emergence of a negative charging energy in a metallic dot capacitively coupled to a superconducting island

C. Holmqvist,[1,2] D. Feinberg,[1] and A. Zazunov[3,4]
[1]*Institut NEEL, Centre National de la Recherche Scientifique, Université Joseph Fourier, Boite Postale 166, 38042 Grenoble, France*
[2]*Applied Quantum Physics Laboratory, MC2, Chalmers University of Technology, S-412 96 Göteborg, Sweden*
[3]*Laboratoire de Physique et Modélisation des Milieux Condensés, CNRS, Université Joseph Fourier, Boite Postale 166, 38042 Grenoble, France*
[4]*Centre de Physique Théorique, CNRS, Université de la Méditerranée, Case 907, Luminy, 13288 Marseille Cedex 9, France*
(Received 18 October 2007; published 27 February 2008)

We consider the hybrid setup formed by a metallic dot, capacitively coupled to a superconducting island *S* connected to a bulk superconductor by a Josephson junction. Charge fluctuations in *S* act as a dynamical gate and overscreen the electronic repulsion in the metallic dot, producing an attractive interaction between two additional electrons. As the offset charge of the metallic dot is increased, the dot charging curve shows charge-skipping positive steps $(+2|e|)$ followed by negative ones $(-|e|)$ signaling the occurrence of a negative differential capacitance. A necessary condition for such an effect is that the capacitance coupling the two islands should be larger than the Josephson junction capacitance. A proposal for experimental detection is given, and potential applications in nanoelectronics are outlined.

DOI: 10.1103/PhysRevB.77.054517 PACS number(s): 74.78.Na, 73.23.Hk

I. INTRODUCTION

At low temperatures, the electronic transport through pointlike metallic nanostructures (quantum dots) is dominated by the electronic Coulomb *repulsion* between additional electrons. When a small-capacitance island is weakly coupled to a normal metallic reservoir, the average number of charges n_N in the island increases one by one with the gate voltage V_{gN}, leading to conductance peaks.[1] This Coulomb blockade phenomenon has recently enabled an individual control of charge or spin, for instance, in view of quantum information protocols.[2,3] We address here the possibility of inverting the sign of the charging energy. Indeed, creating a *negative* (instead of positive) effective charging energy in a normal (nonsuperconducting) metallic island would induce attractive correlations, triggering, for instance, pair tunneling from or to a normal reservoir[4] and a possible charge Kondo effect,[5] or giving rise to bunching correlations, which could be observed in future shot noise experiments.[6–8] Historically, attractive interactions in the solid state are known as valence-skipping states[9] and negative-*U* centers.[10] Another possible mechanism for electronic attraction is mediated by optical phonons, binding two electrons as a bipolaron in confined geometries for strong electron-phonon coupling and medium polarizability.[11] Due to the low polarizability and small effective carrier mass, bipolarons are unlikely to form in a clean GaAs/AlGaAs two-dimensional electron gas (2DEG), although they might do so in the presence of a few donor impurities.[12] More polarizable materials may allow bipolaron formation in a metal and/or polar insulator multilayer.[13] Molecular junctions are also promising for achieving a negative charging energy.[4,14]

In the present work, we propose an alternative mechanism by showing that the repulsive charging energy in a metallic island (*N*) connected to a normal reservoir (Fig. 1) can be turned into an attractive one when *N* is *capacitively* coupled to a superconducting island (*S*). The latter is connected to a superconducting reservoir by a Josephson junction (JJ) and operates in the Cooper pair box regime, e.g., it fluctuates between two pair number states.[15,16] Here, we assume that electron tunneling between *S* and *N* is negligible; therefore, no proximity effect occurs in the *N* island. We instead focus on the charging properties of the *N* island as its gate voltage is varied. The *S* island acts as an effective dynamical gate, whose effects turn out to be nonlinear. As the main result of this work, the Coulomb charging energy in *N* can be overscreened by the neighboring pair fluctuations in *S*, and an effective *local attraction* appears between electrons added into *N*. As a corollary, certain charge states are "skipped" as the *N* gate voltage is varied. The resulting charging curve becomes nonmonotonous, displaying positive steps $(+2|e|)$ followed by negative ones $(-|e|)$. A related effect has been proposed by Averin and Bruder for providing a controlled coupling between two superconducting charge qubits.[17] No-

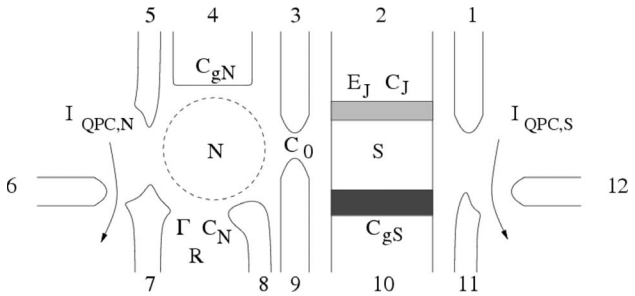

FIG. 1. Schematic view of a normal island (*N*) coupled to a Cooper pair box composed of a Josephson junction connecting superconducting reservoir 2 and island *S*, and gate 10. For strong capacitive coupling (controlled by 3 and 9), *S* imposes an attractive interaction among electrons tunneling between island *N* and its reservoir (defined between 7 and 8). Detection is made by sweeping the gate voltage 4 and measuring the island voltages using quantum point contacts for both *N* (5,6,7) and *S* (1,11,12).

tice that if N were coupled to both drain and source reservoirs, the proposed setup would be similar to a Cooper pair box coupled to a single-electron transistor (SET). The latter has been studied in great detail as a readout device for a superconducting (charge) qubit embodied in the S island.[18] In this case, the capacitive coupling between N and S is assumed to be small, in order to minimize the decoherence due to backaction of the normal part of the device onto the superconducting one, whereas in our proposal, the coupling capacitance is larger than the one of the Josephson junction.

The outline of this paper is as follows. First, the two-island system electrostatics is analyzed in a mean-field picture. It is then coupled to normal and superconducting reservoirs, treating the Josephson term, first as a small perturbation, then by using an adiabatic approximation. We conclude with a discussion of further issues and potential applications.

II. ELECTROSTATIC ANALYSIS

Let us first start with an investigation of the two-island electrostatics. The metallic island, referred to as island N, is coupled to a normally conducting lead by a tunnel junction, whose single-electron tunneling rate is Γ. The electrostatic potential of N can be adjusted by applying a voltage V_{gN} to a gate, with capacitance C_{gN}, which imposes an offset charge of $\nu_N = C_{gN}V_{gN}/e$ in the island. The normal lead has a capacitance $C_N \gg C_{gN}$ and acts as a reservoir for electrons tunneling to island N. Similarly, the superconducting island (S) is connected to a superconducting lead by a Josephson junction with energy E_J. The electrostatic potential of the S island is also determined by a nearby gate with voltage V_{gS} and capacitance C_{gS}, which inflicts an offset charge $\nu_S = C_{gS}V_{gS}/e$ with $C_{gS} \ll C_J$, C_J being the capacitance of the Josephson junction. Most importantly, the islands N and S are coupled by a large capacitance C_0. We assume that the superconducting gap in S is larger than the island's charging energy, such that only even charge number states n_S occur in S. At low temperatures, quasiparticle tunneling in S can be neglected. Defining $C_{\Sigma N} = C_N + C_0 + C_{gN}$ as well as $C_{\Sigma S} = C_J + C_0 + C_{gS}$, and introducing the convenient parameters $b = \frac{C_{\Sigma N}}{C_{\Sigma S}}$ and $r = \frac{C_0}{\sqrt{C_{\Sigma N}C_{\Sigma S}}} < 1$, the total charging energy of the NS system can be written in a standard way as[19]

$$E_C = E_{CN}[(n_N - \nu_N)^2 + b(n_S - \nu_S)^2 + 2r\sqrt{b}(n_N - \nu_N)(n_S - \nu_S)], \tag{1}$$

with $E_{CN} = \frac{e^2}{2C_{\Sigma N}(1-r^2)}$. We similarly define $E_{CS} = \frac{e^2}{2C_{\Sigma S}(1-r^2)}$. Recall that ν_N, ν_S are continuous control parameters. Notice that the asymmetry parameter b and the coupling parameter r are not independent, since both $C_{\Sigma N}$ and $C_{\Sigma S}$ are functions of C_0. In the limit where the coupling capacitance $C_0 \to 0$, the coupling parameter $r \to 0$, too, but b can still take any value in the interval $(0, \infty)$ depending on the capacitance asymmetry of the normal section of the system compared to the superconducting part. On the other hand, in the limit $C_0 \to \infty$, keeping all other capacitances fixed, both parameters $r, b \to 1$. Indeed, increasing r will cause b to approach one, since the only way to increase r is to increase C_0 with respect to all the other capacitances. Specifically, the requirements $r < \sqrt{b}$ for $b \leq 1$ and $r < \frac{1}{\sqrt{b}}$ for $b \geq 1$ have to be fulfilled. Overcoming these limits is unphysical since this would imply negative capacitances.

Equation (1) determines the charge stability diagram of the isolated NS system in the (ν_N, ν_S) plane. A charge stability diagram shows that the combination of charge states (n_N, n_S) minimizes the energy for the system for a certain choice of gate voltages. The lines of degeneracy between two charge states define the hexagons inside which the charge states are stable.

First, for a value ν_S imposing an integer number of pairs in S, say $\nu_S = 2$, the charging number n_N increases monotonously with ν_N. Next, consider a case where n_S fluctuates, for instance, $\nu_S = 1$. For small r, as shown in Fig. 2(a), n_N is again a monotonous function of ν_N: the sequence of charge states (n_N, n_S) as ν_N increases reads (0,0), (0,2), (1,0), (1,2), (2,0), (2,2),… (notice the oscillation of n_S). The charging staircase for island N is plotted in the inset of Fig. 2(a).

Now, assume that r is increased. The slope of the degeneracy lines separating two horizontally neighboring charge states, (n_N, n_S) and (n_N+1, n_S), will become less and less negative. At a certain point, $r = \frac{1}{2\sqrt{b}}$, the transitions between charge states (n_N, n_S) and (n_N+1, n_S+2) will be closed off [Fig. 2(b)] and the charging staircase in the inset of Fig. 2(a) is no longer possible.

If r is increased even further, new transitions between charge states (n_N, n_S+2) and (n_N+2, n_S) open up. These new transitions for large r values result in a very different behavior of the system. In Fig. 2(c), for $\nu_S = 1$, n_N increases with ν_N but in a nonmonotonous way, the charge state sequence being (1,0), (0,2), (2,0), (1,2), (3,0), (2,2), etc. The corresponding charging staircase is plotted in the inset.

At $r = \frac{1}{\sqrt{b}}$, many charge states with the same total number of charges are degenerate [Fig. 2(d)]. From the previous discussion, it is clear that it is not possible to increase r even further in an attempt to create more complex charging staircases.

In the range $\frac{1}{2\sqrt{b}} < r < \frac{1}{\sqrt{b}}$, one sees that the transition from $(n_N, 2)$ to $(n_N+2, 0)$ at $\nu_N = n_N + 1$ "skips" the charge state n_N+1 in the grain. This signals a negative effective charging energy in N which overcomes the Coulomb repulsion. After increasing by two units, n_N decreases by one unit, yielding a negative differential capacitance (NDCA) $C_{diff} = C_{gN}\frac{dn_N}{d\nu_N}$ at half-integer values of ν_N. Strikingly, the total number of steps, positive or negative, is doubled with respect to the usual case. Both charge skipping and NDCA occur above the dotted line indicated in the inset in Fig. 4 displaying a (b, r) diagram. From the above charging energy, an effective attractive potential $U < 0$ can be estimated for $\nu_S = 1$ as $U = E_C(0,2) + E_C(2,0) - 2E_C(1,2) = 2E_{CN}(1 - 2r\sqrt{b})$. The necessary condition for the occurrence of a negative charging energy is thus $2r\sqrt{b} > 1$. It can be rewritten in a more transparent way as $C_0 > C_J + C_{gS}$.

A simple physical understanding of the charge-skipping behavior can be gained from realizing that in the large coupling limit, the two islands tend to behave as a one-island

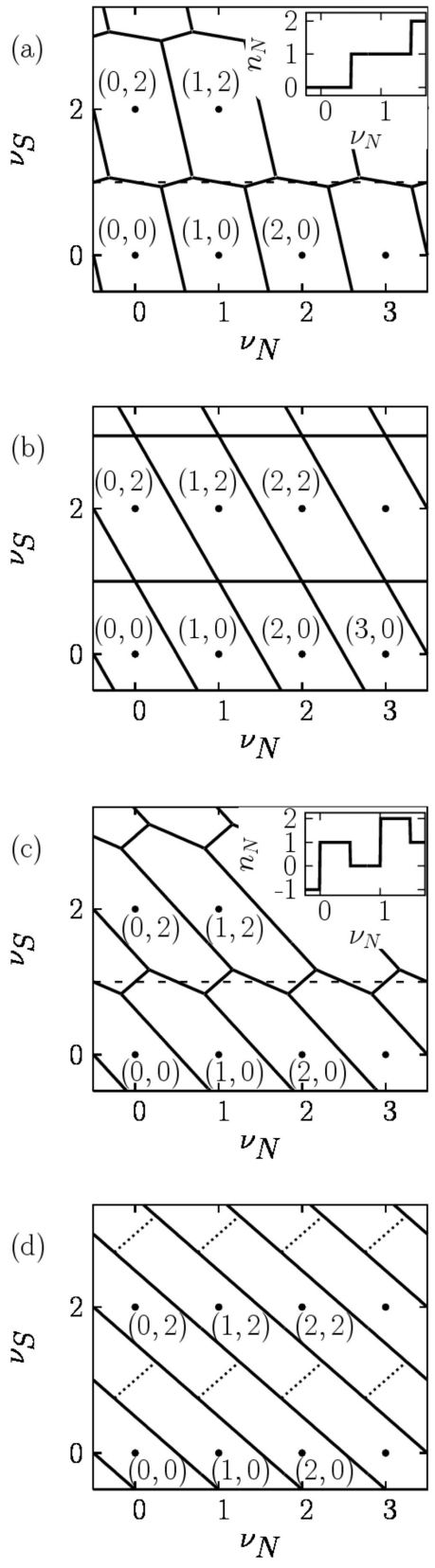

FIG. 2. Charge stability (or honeycomb) diagram for $b=1$, (a) $r=0.2$, (b) $r=0.5$, (c) $r=0.8$, and (d) $r=1$. The insets show the charging curves for N. In case (c), the charging staircase (inset) exhibits charge-skipping effects.

system. The consequence is that it does not matter energy wise if there are two charges in the form of a Cooper pair sitting on the S island or if there are two electrons in the N island—the two cases are electrostatically equivalent. This shows that pairing in S is essential to achieve charge skipping in N. The latter indeed results from strong capacitive coupling between the charge in N and the charge being even in S, and it could not be obtained in a pair of normal metallic islands.

III. CHARGE DYNAMICS OF THE DOUBLE-ISLAND SYSTEM

To further analyze this possibility in an open NS system, let us consider the full Hamiltonian,

$$H = \hat{E}_C + \sum_{k\sigma} \varepsilon_k c^\dagger_{kR,\sigma} c_{kR,\sigma} + \sum_{q\sigma} \varepsilon_q c^\dagger_{qN,\sigma} c_{qN,\sigma} + \left[\sum_{kq\sigma} T_{k,q} c^\dagger_{kR,\sigma} c_{qN,\sigma} - \frac{E_J}{2} |n_S + 2\rangle\langle n_S| + \text{H.c.} \right], \quad (2)$$

where k (q) denotes electron states in the normal reservoir R (island N) and $T_{k,q}$ is a tunnel matrix element. The Coulomb operator $\hat{E}_C$ is obtained from Eq. (1) by replacing the occupation numbers n_N, n_S by operators $\hat{n}_N$, $\hat{n}_S$, and E_J is the Josephson energy. The total charge in N is expressed as $\hat{n}_N = \Sigma_{q\sigma} c^\dagger_{qN,\sigma} c_{qN,\sigma}$. Assuming for simplicity the constant densities of states ρ_R, ρ_N in R and N, and $|T_{kq}| = T$, the single-electron transition rate from R to N is given by $\Gamma^{(+1)} = \frac{\delta E_C^{(+1)}}{e^2 R_N} [\exp(\delta E_C^{(+1)}/k_B T) - 1]^{-1}$ within the golden rule approximation, where R_N is the tunnel resistance, expressed as $\frac{1}{R_N} = \frac{2e^2}{h}(2\pi)^2 |T|^2 \rho_R \rho_N \Omega_R \Omega_N$. The index (+1) indicates that one electron is added to the dot N, and $\Omega_{R/N}$ is the volume of the lead and island.

A. Small Josephson energy

Considering first the case of small $E_J \ll E_{CS}$, we perform a T-matrix calculation of the transition rates from (0,2) to (2,0) (close to $\nu_N = 1$) and from (2,0) to (1,2) (close to $\nu_N = 1.5$). For the first transition, we take into account three possible configuration paths involving higher-energy states: $(0,2) \to (1,2) \to (2,2) \to (2,0)$, $(0,2) \to (1,2) \to (1,0) \to (2,0)$, and $(0,2) \to (0,0) \to (1,0) \to (2,0)$. For the second transition, only one excited state is involved: $(2,0) \to (1,0) \to (1,2)$ and $(2,0) \to (2,2) \to (1,2)$. Denoting by H_T the tunneling term from R [fourth term in Hamiltonian (2)], the Josephson term by H_J, and setting $H_0 = H - H_T - H_J$, the second- and third-order T-matrix operators are

$$T^{(2)} = (H_T + H_J) \frac{1}{E_0 - H_0} (H_T + H_J) \quad (3)$$

and

$$T^{(3)} = (H_T + H_J) \frac{1}{E_0 - H_0} (H_T + H_J) \frac{1}{E_0 - H_0} (H_T + H_J). \quad (4)$$

Then, the tunneling rate from the initial to the final state is calculated as $\Gamma(i \to f) = \frac{2\pi}{\hbar} |\langle f|T|i\rangle|^2 \delta(E_i - E_f)$. The shape of

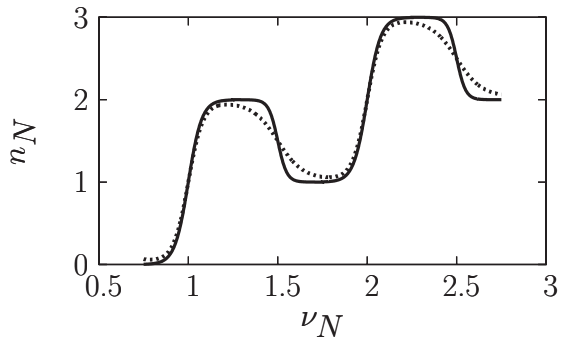

FIG. 3. Charging staircase: (i) (full line) perturbative solution in E_J for $r=0.8$, $b=1$, $E_J/E_{CS}=0.5$, $k_BT/E_{CS}=3\times10^{-2}$, and $R_N/R_K=10$; (ii) (dotted line) adiabatic solution for $E_J/E_{CS}=2$, the other parameters being unchanged.

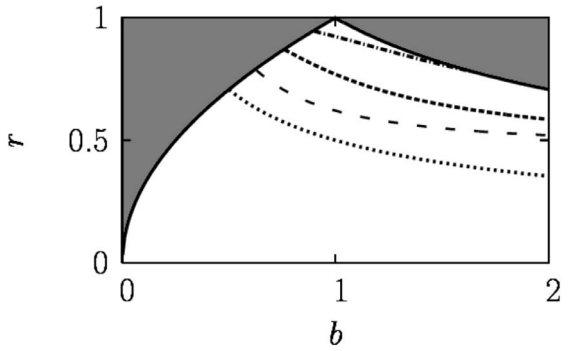

FIG. 4. Phase diagram in the b,r plane. The unphysical gray region is excluded. Charge skipping and NDCA occur above the dotted line from bottom to top: $E_J/E_{CS}=0$ (analytic), 1, 2, and 4 (adiabatic calculation). All other parameters are the same as in Fig. 3.

each step is obtained at finite temperature by solving the master equation governing the dynamics of the probabilities $p(0,2)$, $p(2,0)$ for the positive step and $p(2,0)$, $p(1,2)$ for the negative one. The master equation reads as usual $\dot{p}(a)=\Gamma^{b\to a}p(b)-\Gamma^{a\to b}p(a)$, with $p(b)=1-p(a)$ for the states a,b involved in the transition. Here, the probabilities of other states are neglected, which is justified close to $\nu_N=1$ or $\nu_N=1.5$ and if the steps are sufficiently narrow. The resulting steps are shown in Fig. 3.

As a result, a positive step $+2|e|$ (where the charge number $n_N=1$ is skipped) and a consecutive negative step $-|e|$ are stabilized. Notice that contrary to the usual staircase, where all transitions between n and $n\pm1$ are real and treated by the same master equation,[20] here the rates are of higher order and the virtual states involved in one transition (positive step) become real states (with first-order rates) for the next (negative) one. A full treatment of all processes is beyond the scope of this paper.

B. Large Josephson energy

Let us now turn to the case of a large Josephson energy. Then, one can resort to an adiabatic approximation.[17] It amounts to assume a slow variation of the charge number in N which modulates the effective gate voltage acting on the superconducting island. It requires that all the energy scales characterizing such a dynamics, including the single- and two-electron transition rates connecting different charge states in N, be much smaller than E_J. Then, the Cooper-pair box operates phase coherently, which amounts to neglect transitions between the Bloch bands.[15] Setting the phase difference to ϕ across the JJ, and neglecting the normal electron tunneling term, yields the resulting adiabatic Hamiltonian,

$$H_{ad}=E_{CN}(n_N-\nu_N)^2+E_{CS}\left[(\hat{n}_S-\nu_S)^2+2\frac{r}{\sqrt{b}}(n_N-\nu_N)(\hat{n}_S-\nu_S)\right]-E_J\cos\phi. \tag{5}$$

Apart from the first term, this Hamiltonian represents a Cooper-pair box submitted to an effective gate depending on the charge n_N. In the tight-binding limit $\frac{E_J}{E_{CS}}\gg1$, assuming that the junction dynamics is confined to the lowest Bloch band, one obtains the sum of the N dot charging energy and the adiabatic Bloch band energy,

$$E_{ad}=E_{CN}(1-r^2)(n_N-\nu_N)^2-\Delta_0\cos\left[\pi\left(\nu_S-\frac{r}{\sqrt{b}}(n_N-\nu_N)\right)\right], \tag{6}$$

where the bandwidth is given by[15]

$$\Delta_0=16\sqrt{\frac{2}{\pi}}E_{CS}\left(\frac{E_J}{2E_{CS}}\right)^{3/4}e^{-\sqrt{8E_J/E_{CS}}}. \tag{7}$$

Here, E_{ad} appears as an effective charging energy for the N island, depending on the additional parameter ν_S. The second term in E_{ad} represents a nonlinear screening potential acting on the charge in N. The gate offset ν_S controls the phase of the cosine term, and an appropriate choice (for instance, $\nu_S\approx1$) allows us to achieve a negative curvature of E_{ad}. The required condition reads $\frac{\pi^2}{2}\frac{r^2}{b(1-r^2)}\Delta_0>1$, yielding the lines in Fig. 4. Clearly, a large E_J sets a stronger constraint on the coupling capacitance C_0 and requires values of r closer to one than for smaller E_J values. The shape of the charge skipping and negative steps is then calculated like in Sec. II, using a master equation based on transition rates between charge states $n_N=0,2$ or $n_N=2,1$, respectively. The adiabatic transition rates are given by $\Gamma_{ad}=\frac{\delta E_{ad}}{e^2R_N}[\exp(\delta E_{ad}/k_BT)-1]^{-1}$. The corresponding steps are shown in Fig. 3 (dotted line) and are less pronounced than in the small E_J case.

IV. DISCUSSION

Searching for the optimum regime must account for the fact that for too large r values, the system behaves like one single island and its energy no longer depends on the location of the charge. Operating in the Coulomb blockade regime requires temperatures much smaller than the energy difference between two charge states. As a result, for, say

$b=1$, an optimal r is close to 0.75 for small Josephson energies. In this case, the requirement for Coulomb blockade is $k_BT<\frac{E_{CN}}{4}$. In the step calculations, the value $r=0.8$ was used to accommodate for both the small and large Josephson energy cases. A temperature $T\sim 30$ mK and a typical charging energy $E_{CN}\sim 0.1$ meV were used. For the symmetric case ($b=1$), this charging energy gives $C_N=C_J\sim 2$ fF. Furthermore, if we assume, e.g., $C_{gN}=C_{gS}=0.02$ fF, then the offset charges $\nu_S=1$ and $\nu_N=0.75-2.75$ correspond to $V_{gS}=4$ mV and $V_{gN}=6-22$ mV, respectively. The value of r chosen for the calculations corresponds to $C_0=4C_N=8$ fF. Recently, coupling values as high as $r=0.35$ were achieved in lateral normal dots.[21] Notice that such a value is sufficient for our purpose if b is larger than 5.

An additional requirement for Coulomb blockade is that the tunnel resistance R_N be larger than the resistance quantum $R_K=\frac{h}{e^2}\approx 25.8$ kΩ. The value $\frac{R_N}{R_K}=10$ was used, yielding a bare single-electron tunneling rate of $\Gamma\sim 10^9$ s^{-1}, obtained in the absence of S. In the presence of the S island, the effective tunneling rates are 10^7 s^{-1} (n_N decreasing from 2 to 1) and 5×10^3 s^{-1} (n_N increasing from 0 to 2), respectively. With the above parameters, the maximum attraction $|U|$ is of the order of 40 μeV. This allows operation of the device at cryogenic dilution temperatures. Higher temperatures could be reached by decreasing the size of the device elements, thus increasing the Coulomb energy scales. Carbon nanotubes or even molecular units could be envisioned.

One might wonder whether such a negative charging energy may render the dot superconducting. It is not the case because it concerns the energy required to add one or two electrons on the dot rather than a true attractive potential felt by all electrons near the Fermi level. The effective "negative-U" potential manifests itself only when the dot is weakly coupled to a reservoir such that its charge can fluctuate. The situation is indeed very similar to a single "$-U$" center weakly hybridized with an otherwise normal bulk metal. In the present case, pair fluctuations with the reservoir are assumed to be incoherent. On the contrary, a very small tunneling term T_{NS} between N and S would open the possibility of establishing a true phase coherence between states n_N, n_N+2. Then, the proximity effect could be studied in a quite unusual regime, where $T_{NS}<|U|$.

Let us briefly discuss the issue of phase coherence in the Cooper-pair box. As shown above, charge skipping only requires that pair tunneling occurs between the superconducting reservoir and the S island in order to screen the repulsive interaction in the normal grain. No phase coherence is needed, as shown by the first calculation performed in the small E_J case. Moreover, even in the large E_J case, charge fluctuations in N should strongly react back upon S and reduce the phase coherence. A full treatment goes beyond the adiabatic approximation.[22] One can anticipate that corrections to the adiabatic behavior cause substantial fluctuations in the phase ϕ, renormalizing E_J to a smaller value, thus making the small-E_J case generic.

We now propose a scheme for detecting an induced attraction in a normal metallic grain. The goal is to detect the nonmonotonous charging of the N grain. SETs or point contacts[23] provide very sensitive detection of the local change in the electrostatic potential (rather than the charge). In double-dot setups with weak mutual coupling, the potential variations in each dot can be measured by a different neighboring point contact.[24] In the present case, placing a point contact close to N does not measure δn_N, but instead $\delta V_N=(C^{-1})_{NN}(e\,\delta n_N)+(C^{-1})_{NS}(e\,\delta n_S)=\frac{2E_{CN}}{e}[\delta n_N+r\sqrt{b}\,\delta n_S]$, where $(C^{-1})_{NN}=\frac{C_{\Sigma S}}{C_{\Sigma N}C_{\Sigma S}-C_0^2}$ and $(C^{-1})_{NS}=\frac{C_0}{C_{\Sigma N}C_{\Sigma S}-C_0^2}$ are coefficients of the inverse capacitance matrix. If $C_0>C_J+C_{gS}$, doubling of the number of steps can be detected this way, but not the nonmonotonous charging curve. To access the latter, it is suitable to measure $\delta V_S=\frac{2E_{CN}}{e}[r\sqrt{b}\,\delta n_N+b\,\delta n_S]$ as well, with a second point contact close to S [Fig. 1], and reconstruct $\delta n_N=\frac{C_{\Sigma N}}{e}\left[\delta V_N-\frac{r}{\sqrt{b}}\delta V_S\right]$. The parameters $C_{\Sigma N}$, r, and b can easily be measured from the stability diagram obtained in the normal (nonsuperconducting) state in the presence of a very weak tunneling between N and S.[19] Notice that the tunneling rates calculated above are much reduced compared to the bare single-electron rate Γ. Therefore, the use of point contacts permits not just a time averaged[24] but even a time resolved and directional[25] detection of the charge variations in N and S. On the other hand, cross-correlation shot noise measurements, as in Ref. 26, would require higher currents. In practice, a possible setup inspired by Ref. 24 is proposed in Fig. 1. It involves a superconducting strip with a Cooper-pair box, coupled laterally to an InGaAs/AlGaAs 2DEG, suitably tuning the barrier present at the interface between the superconductor and the 2DEG.

Going beyond the single dot case, the same mechanism could establish attractive correlations between electrons in spatially *separated* normal dots (similar to the all-superconducting case of Ref. 17). This could be useful for implementing quantum information protocols involving two-qubit gates, when the qubits are carried by the charge (spin) of the last added electron. Indeed, two electrons coming from the same or from separate quantum wires could be simultaneously captured in a pair of dots and undergo a quantum gate, acting, for instance, on their spin degrees of freedom.

In conclusion, we have proposed a mechanism inducing a controllable negative charging energy, thus attractive correlations, in one or several metallic dots. Besides its intrinsic interest, such an effect would be useful in view of more complex nanoelectronic devices.

ACKNOWLEDGMENTS

The authors are grateful to T. Martin, C. Bruder, M. Fogelström, and G. Johansson for useful discussions and S. Andergassen for careful reading of the paper. D. F. and A. Z. were partially supported by the Contract No. AC NANO NR0114. The work of C.H. was supported by the Swedish Research Council (VR) under Grant No. 621-2006-3072.

[1] H. van Houten and C. W. J. Beenakker, Phys. Rev. Lett. **63**, 1893 (1989); D. V. Averin, A. N. Korotkov, and K. K. Likharev, Phys. Rev. B **44**, 6199 (1991); M. A. Kastner, Rev. Mod. Phys. **64**, 849 (1992).

[2] T. Hayashi, T. Fujisawa, H. D. Cheong, Y. H. Jeong, and Y. Hirayama, Phys. Rev. Lett. **91**, 226804 (2003).

[3] P. Recher, E. V. Sukhorukov, and D. Loss, Phys. Rev. Lett. **85**, 1962 (2000); R. Hanson, L. H. Willems van Beveren, I. T. Vink, J. M. Elzerman, W. J. M. Naber, F. H. L. Koppens, L. P. Kouwenhoven, and L. M. K. Vandersypen, *ibid.* **94**, 196802 (2005).

[4] J. Koch, M. E. Raikh, and F. von Oppen, Phys. Rev. Lett. **96**, 056803 (2006).

[5] A. Taraphder and P. Coleman, Phys. Rev. Lett. **66**, 2814 (1991); P. S. Cornaglia, H. Ness, and D. R. Grempel, *ibid.* **93**, 147201 (2004).

[6] J. Koch, E. Sela, Y. Oreg, and F. von Oppen, Phys. Rev. B **75**, 195402 (2007).

[7] M.-J. Hwang, M.-S. Choi, and R. López, Phys. Rev. B **76**, 165312 (2007).

[8] O. Sauret and D. Feinberg, Phys. Rev. Lett. **92**, 106601 (2004).

[9] C. M. Varma, Phys. Rev. Lett. **61**, 2713 (1988).

[10] P. W. Anderson, Phys. Rev. Lett. **34**, 953 (1975).

[11] E. P. Pokatilov, V. M. Fomin, J. T. Devreese, S. N. Balaban, and S. N. Klimin, J. Phys.: Condens. Matter **11**, 9033 (1999).

[12] Yi Wan, G. Ortiz, and P. Phillips, Phys. Rev. Lett. **75**, 2879 (1995).

[13] E. P. Pokatilov, S. I. Beril, V. M. Fomin, and G. Yu. Ryabukhin, Phys. Status Solidi B **169**, 429 (1992).

[14] A. S. Alexandrov, A. M. Bratkovsky, and R. S. Williams, Phys. Rev. B **67**, 075301 (2003).

[15] K. K. Likharev and A. B. Zorin, J. Low Temp. Phys. **59**, 347 (1985); for a review, see D. V. Averin and G. Schön, in *Quantum Coherence in Mesoscopic Systems*, edited by B. Kramer (Plenum, New York, 1991), p. 531.

[16] M. Büttiker, Phys. Rev. B **36**, 3548 (1987); V. Bouchiat, P. Joyez, H. Pothier, C. Urbina, D. Estève, and M. H. Devoret, Phys. Scr., T **T76**, 165 (1998).

[17] D. V. Averin and C. Bruder, Phys. Rev. Lett. **91**, 057003 (2003).

[18] A. Aassime, G. Johansson, G. Wendin, R. J. Schoelkopf, and P. Delsing, Phys. Rev. Lett. **86**, 3376 (2001); for a review, see G. Wendin and V. S. Shumeiko, in *Handbook of Theoretical and Computational Nanotechnology*, edited by M. Rieth and W. Schommers (American Scientific, Stevenson Ranch, CA, 2006).

[19] H. Pothier, P. Lafarge, C. Urbina, D. Esteve, and M. H. Devoret, Europhys. Lett. **17**, 249 (1992); for a review, see W. G. van der Wiel, S. De Franceschi, J. M. Elzerman, T. Fujisawa, S. Tarucha, and L. P. Kouwenhoven, Rev. Mod. Phys. **75**, 1 (2003).

[20] C. W. J. Beenakker, Phys. Rev. B **44**, 1646 (1991).

[21] A. Hübel, J. Weis, W. Dietsche, and K. v. Klitzing, Appl. Phys. Lett. **91**, 102101 (2007).

[22] C. Hutter, A. Shnirman, Y. Makhlin, and G. Schön, Europhys. Lett. **74**, 1088 (2006).

[23] M. Field, C. G. Smith, M. Pepper, D. A. Ritchie, J. E. F. Frost, G. A. C. Jones, and D. G. Hasko, Phys. Rev. Lett. **70**, 1311 (1993).

[24] L. DiCarlo, H. J. Lynch, A. C. Johnson, L. I. Childress, K. Crockett, C. M. Marcus, M. P. Hanson, and A. C. Gossard, Phys. Rev. Lett. **92**, 226801 (2004).

[25] T. Fujisawa, T. Hayashi, R. Tomita, and Y. Hirayama, Science **312**, 1634 (2006).

[26] D. T. McClure, L. DiCarlo, Y. Zhang, H.-A. Engel, C. M. Marcus, M. P. Hanson, and A. C. Gossard, Phys. Rev. Lett. **98**, 056801 (2007).